FGF21 regulates PGC-1α and browning of white adipose tissues in adaptive thermogenesis

ffolliott M. Fisher,[1,5] Sandra Kleiner,[2,3,5] Nicholas Douris,[1] Elliott C. Fox,[1] Rina J. Mepani,[2,3] Francisco Verdeguer,[2,3] Jun Wu,[2,3] Alexei Kharitonenkov,[4] Jeffrey S. Flier,[1] Eleftheria Maratos-Flier,[1,6] and Bruce M. Spiegelman[2,3,6]

[1]Department of Medicine, Beth Israel Deaconess Medical Center, Harvard Medical School, Boston, Massachusetts 02215, USA; [2]Department of Cell Biology, [3]Department of Cancer Biology, Division of Metabolism and Chronic Disease, Dana-Farber Cancer Institute, Harvard Medical School, Boston, Massachusetts 02115, USA; [4]Lilly Research Laboratories, Eli Lilly and Company, Indianapolis, Indiana 46285, USA

Certain white adipose tissue (WAT) depots are readily able to convert to a "brown-like" state with prolonged cold exposure or exposure to β-adrenergic compounds. This process is characterized by the appearance of pockets of uncoupling protein 1 (UCP1)-positive, multilocular adipocytes and serves to increase the thermogenic capacity of the organism. We show here that fibroblast growth factor 21 (FGF21) plays a physiologic role in this thermogenic recruitment of WATs. In fact, mice deficient in FGF21 display an impaired ability to adapt to chronic cold exposure, with diminished browning of WAT. Adipose-derived FGF21 acts in an autocrine/paracrine manner to increase expression of UCP1 and other thermogenic genes in fat tissues. FGF21 regulates this process, at least in part, by enhancing adipose tissue PGC-1α protein levels independently of mRNA expression. We conclude that FGF21 acts to activate and expand the thermogenic machinery in vivo to provide a robust defense against hypothermia.

Brown adipose tissue (BAT) is a specialized tissue that dissipates chemical energy to protect against hypothermia and obesity through a process termed nonshivering thermogenesis. Active BAT burns lipids to produce heat, resulting in an increase in energy expenditure. Many studies have shown that changes in BAT activity can profoundly affect body weight and glucose homeostasis (Lowell et al. 1993; Kopecky et al. 1995; Cederberg et al. 2001; Feldmann et al. 2009). Cold exposure activates the sympathetic nervous system, resulting in the stimulation of β-adrenergic receptors on brown adipocytes. This process induces mitochondrial uncoupling protein 1 (UCP1), which uncouples oxidative phosphorylation from ATP production, releasing chemical energy as heat. The expression of *UCP1* is driven by several transcriptional components, including the coactivator PGC-1α, which is strongly induced by cold exposure and/or β-adrenergic signaling

(Barbera et al. 2001). Additionally, PGC-1α regulates oxidative metabolism by coordinately increasing mitochondrial gene expression and function (Wu et al. 1999). *PGC-1α* and *UCP1* are highly expressed in BAT, which contains multilocular adipocytes enriched with mitochondria.

It is now clear that there are two distinct types of brown adipose cells. One is the classical brown fat that arises from a myf5, muscle-like cell lineage (Seale et al. 2008; Lepper and Fan 2010). This is exemplified by the interscapular BAT depots and the perirenal BAT depot, a depot that contains a mixture of classical brown and white adipocytes (Seale et al. 2008; Cinti 2009). In addition, UCP1-positive, brown fat-like cells can emerge in most white fat (white adipose tissue [WAT]) depots upon prolonged cold exposure or β-adrenergic receptor activation (Cousin et al. 1992; Ghorbani and Himms-Hagen 1997; Barbatelli et al. 2010). These brown fat cells, which are not derived from a myf5-positive lineage, are designated beige or brown-in-white (brite) cells (Petrovic et al. 2010; Seale et al. 2011). The propensity to accumulate brite/beige cells differs between WAT depots in rodents. A large accumulation of brown-like cells during cold exposure can be found most readily in the subcutaneous inguinal

[5]These authors contributed equally to this work.
[6]Corresponding authors.
E-mail bruce_spiegelman@dfci.harvard.edu.
E-mail emaratos@bidmc.harvard.edu.

adipose tissue, but is rather seldom observed in epididymal/perigonadal adipose tissue (Seale et al. 2011). Notably, an increase in the abundance of brite/beige cells in WAT ("browning") has been observed in a large number of knockout (KO) strains that show resistance to diet-induced obesity and improved glucose metabolism (Tsukiyama-Kohara et al. 2001; Hansen et al. 2004; Christian et al. 2005; Wang et al. 2008; Romanatto et al. 2009).

Fibroblast growth factor 21 (FGF21) has emerged as an important regulator of metabolic processes (Kharitonenkov et al. 2005; Badman et al. 2007; Inagaki et al. 2007). Systemic administration and transgenic overexpression of this factor leads to weight loss in obese mouse models through increases in energy expenditure without alterations in food intake (Kharitonenkov et al. 2005; Coskun et al. 2008). Thus far, the known target tissues of FGF21 action are liver, epididymal WAT (Fisher et al. 2010), and the pancreas (Wente et al. 2006; Johnson et al. 2009). The hepatic effects of FGF21 are dramatic, leading to increased fatty acid oxidation (Coskun et al. 2008; Potthoff et al. 2009). Although FGF21 was originally found to stimulate insulin-independent glucose uptake in adipocytes through induction of *GLUT1* expression (Kharitonenkov et al. 2005; Moyers et al. 2007) and to inhibit liploysis (Arner et al. 2008; Li et al. 2009), little is known about further functions of FGF21 in adipose tissue (Kharitonenkov et al. 2005).

We recently showed that both BAT and WAT express high levels of the critical coreceptor *β-klotho* and are sensitive to exogenous FGF21 stimulation (Fisher et al. 2011). FGF21-KO mice have larger BAT depots containing larger lipid droplets, suggesting a function for FGF21 in this tissue (Badman et al. 2009). In addition, two recent reports demonstrated that FGF21 is synthesized in BAT in response to cold exposure and β-adrenergic stimulation; however, little effect of either stimulation was observed on visceral WAT depots (Chartoumpekis et al. 2011; Hondares et al. 2011).

Since FGF21 increases energy expenditure and is expressed in cold-stimulated BAT, we investigated in detail the role of FGF21 in regulating the thermogenic activity of adipose tissue. Here we show that FGF21 treatment stimulates *UCP1* gene expression in both BAT and WAT. It dramatically increases the appearance of brown-like adipocytes in subcutaneous WAT. Moreover, FGF21 plays an important role in the cellular and molecular adaptation of adipose tissues to cold exposure. Interestingly, FGF21 does not regulate *PGC-1α* mRNA levels but post-transcriptionally increases the protein content of this key regulatory protein in adipose tissue.

Results

Pharmacologic treatment of FGF21 induces thermogenic gene expression and browning of WAT

FGF21 is a critical regulator of fatty acid oxidation in the liver during periods of nutritional deprivation or consumption of a ketogenic diet (Inagaki et al. 2007; Badman et al. 2009). However, the role of FGF21 in adipose tissue function remains poorly understood. Since BAT uses fatty acids as fuel for nonshivering thermogenesis, we investigated whether FGF21 affects the thermogenic activity of adipose tissue. In BAT, 3-d infusion of FGF21 mildly increased expression of key thermogenic genes *UCP1* and *DIO2* (Fig. 1A). In addition, FGF21 increased the expression of *CPT1α* and *CPT1β*, similar to what has been described in the liver and consistent with the idea that FGF21 mobilizes fatty acid usage. Interestingly, a much greater induction of thermogenic gene expression occurred in the inguinal WAT (IWAT) (Fig. 1B). FGF21 administration resulted in a 20-fold increase in *UCP1*
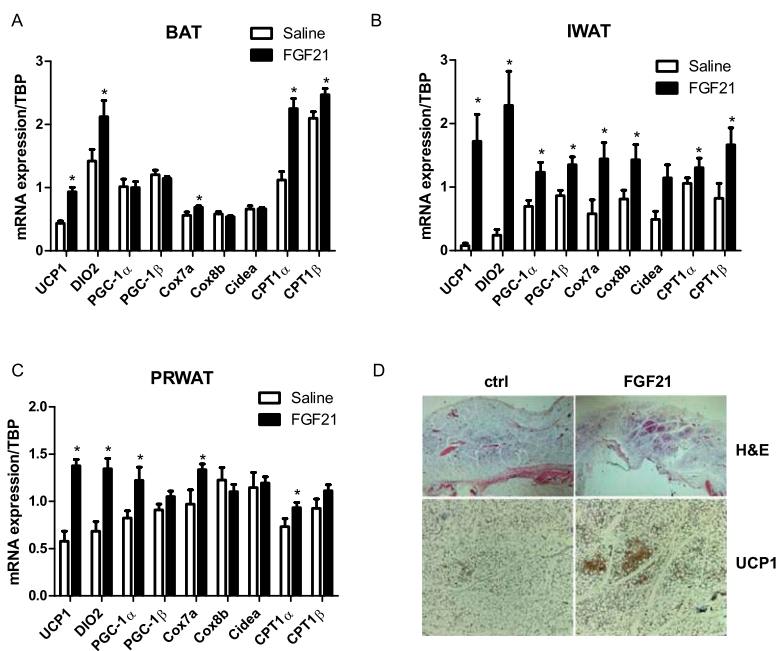

Figure 1. FGF21 induces adipose thermogenic gene expression and browning of WAT. Mice were chronically treated with saline ($n = 7$) or FGF21 ($n = 9$) for 72 h. Real-time PCR analysis of thermogenic gene expression is shown from BAT (*A*), IWAT (*B*), and PRWAT (*C*). (*D*) H&E and UCP1 immunostaining in IWAT. Data are shown ±SEM; saline versus FGF21, (*) $P < 0.05$.

expression and a 10-fold increase in *DIO2* expression in this depot. Notably, molecular markers of brown-like adipocytes, such as *CIDEA* and *Cox7a*, were also significantly increased. Additionally, we observed a 1.4-fold increase in *PGC-1α* mRNA levels in IWAT of FGF21-treated mice (Fig. 2B). A similar induction of gene expression was seen in perirenal adipose tissue (PRWAT), which consists of a mixture of myf5-positive brown adipocytes and classical white adipocytes (Fig. 1C; Seale et al. 2008). The observed induction of genes characteristic of brown/beige fat suggested an overall browning of these adipose tissues. Indeed, the histology revealed a substantial increase in the appearance of pockets of multilocular, UCP1-expressing adipocytes in the IWAT of FGF21-treated animals (Fig. 1D). FGF21 also induced *UCP1* and *DIO2* expression in epididymal WAT (EWAT); however, even the induced levels of these genes were insignificant compared with the expression levels observed in IWAT and PRWAT (Supplement Fig. 1A,C). In addition, we did not see an increase in the expression of markers of brown adipocytes (*CIDEA*, *Cox8b*, and *Cox7a*), nor did we observe the histological appearance of any "brown-like" adipocytes in EWAT (data not shown).

To investigate whether these alterations in gene expression were mediated by an indirect effect or are direct effects on the adipocytes, we treated primary BAT, IWAT, and EWAT adipocytes with FGF21 and assessed the patterns of thermogenic gene expression. A 2-d FGF21 treatment induced *UCP1* and *CIDEA* mRNAs twofold to fourfold in differentiated brown, inguinal, and epididymal white adipocytes (Fig. 2A–C). *CPT1α* and *CPT1β* mRNA levels were also increased in brown and inguinal white adipocytes, similar to that observed in vivo. The extent of differentiation was not visibly affected by FGF21 treatment, and general adipose differentiation genes such as aP2 were not altered. Interestingly, we did not observe an

increase in *PGC-1α*, *Cox7a*, and *Cox8b* mRNA levels in any of these cultures. Taken together, these data demonstrate that FGF21 can induce thermogenic gene expression and augmentation of a brown fat-like phenotype in white adipose cells and tissues.

FGF21 expression is induced by cold exposure and β-adrenergic stimulation in BAT and thermogenically competent WAT depots

Thermogenic activation of brown and beige fat is critical in the adaptive response to cold environments. In addition, two recent reports demonstrated that FGF21 mRNA expression is induced in classical BAT upon cold stimulus (Chartoumpekis et al. 2011; Hondares et al. 2011). We therefore analyzed the expression of *FGF21* in adipose tissue depots during a cold challenge. Indeed, a robust induction of *FGF21* mRNA expression (threefold) was observed in BAT after 3 d of cold exposure (Fig. 3A). Furthermore, *FGF21* mRNA levels were also increased dramatically in the WAT tissue depots that have an enhanced capacity to convert to a "brown-like" state, such as IWAT (fivefold) and PRWAT (16-fold) (Fig. 3A). Notably, the visceral depot EWAT, which has a low thermogenic capacity, does not express higher levels of *FGF21* as a consequence of cold exposure. Increased *FGF21* expression in adipose tissue was evident with as little as 6 h of cold exposure (data not shown). Cold-induced *FGF21* expression was restricted to the adipose tissues as *FGF21* mRNA levels decreased in the liver, in contrast to the observed cold-induced gluconeogenic gene expression (Fig. 3B). Importantly, the enhanced expression of *FGF21* mRNA in WAT and BAT did not lead to increased circulating levels of FGF21 (Fig. 3C). Additionally, adipose *FGF21* mRNA levels also increased upon CL316243 injection, confirming that expression is regulated by β3-adrenergic signaling (Fig. 3D).
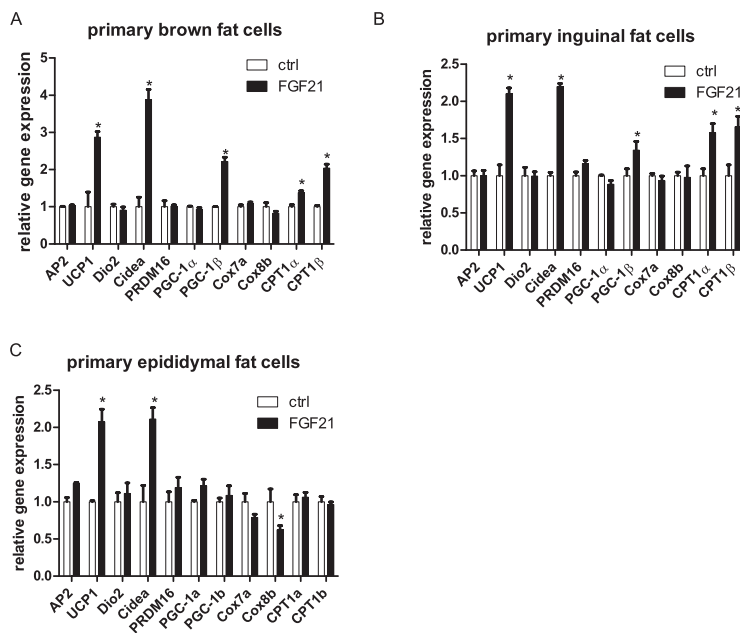

Figure 2. FGF21 regulates thermogenic gene expression in primary WAT and BAT adipocytes. Differentiated primary adipocytes were treated with 50 nM FGF21 for 48 h. Gene expression profiles are shown from adipocytes sourced from BAT (*A*), IWAT (*B*), and EWAT (*C*). Data are shown ±SEM; control versus FGF21, (*) $P < 0.05$.
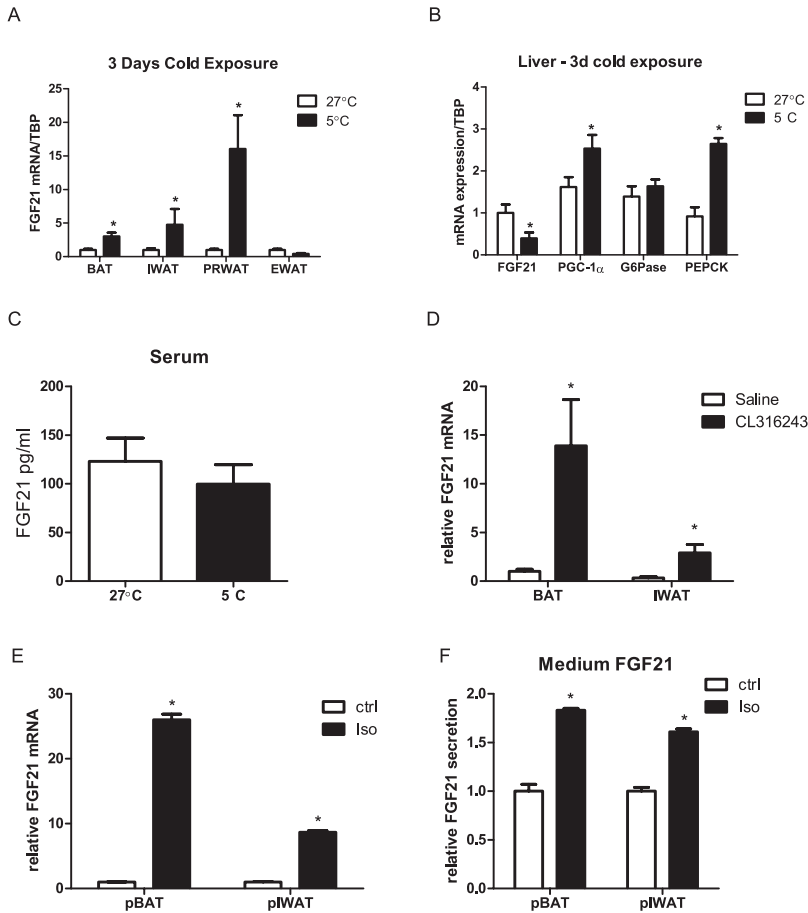
Fisher et al.

Figure 3. Adipose FGF21 expression and secretion are regulated by cold exposure and β3-adrenergic signaling. Wild-type mice were kept for a 72-h period at 5°C, and tissues were subsequently dissected for further analysis. (*A*) FGF21 mRNA expression in multiple adipose tissue depots following cold exposure; 5°C ($n = 5$) versus 27°C ($n = 5$), (*) $P < 0.05$. Hepatic FGF21 and gluconeogenic gene expression (*B*) and FGF21 serum (*C*) levels. The effect of β-adrenergic stimulation on adipose FGF21 expression in mice (*D*) (saline vs. CL316243, [*] $P < 0.05$) and primary adipocytes (*E*). (*F*) Medium FGF21 levels from primary adipocytes treated with isoproterenol; saline versus isoproterenol, (*) $P < 0.05$. Data are shown ±SEM.

To verify that FGF21 is synthesized and secreted by adipocytes, we treated differentiated primary brown and inguinal white adipocytes with isoproterenol (β-agonist). *FGF21* mRNA levels were robustly increased 6 h post-treatment in differentiated primary BAT (26-fold) and IWAT (ninefold) adipocytes (Fig. 3E). Increased FGF21 levels were also found in the medium of isoproterenol-treated primary adipocytes (Fig. 3F), indicating that adipocytes are indeed capable of synthesizing and secreting FGF21. This suggests that adipose FGF21 may act mainly in a paracrine/autocrine manner. These data show that *FGF21* gene expression is induced in adipocytes upon cold stimulus and is linked to the endogenous thermogenic response.

Genetic ablation of FGF21 leads to an impaired adaptation to cold exposure

We next asked whether FGF21 is required for cold-induced adaptive thermogenesis. To do this, we exposed FGF21-KO mice to an ambient temperature of 5°C for 3 d. Mice were implanted with telemetry probes to continuously monitor core body temperature. At temperatures close to thermoneutral (27°C), when adaptive thermogenesis is not required, gene expression and morphology were very similar between wild-type and FGF21-KO mice (Fig. 4E). However, robust differences were apparent after a 3-d cold exposure. The FGF21-KO mice were colder than their wild-type littermates by ~0.5°C through-

out the duration of the experiment, although this effect did not reach statistical significance ($P = 0.057$) (Fig. 4A). FGF21-KO mice were less active during cold exposure and had increased circulating creatine kinase activity levels (Supplemental Fig. 2A,B), which is indicative of enhanced shivering (Cannon and Nedergaard 2011). Although differences in cold-induced thermogenic gene expression was not apparent in the intersacpular BAT of FGF21-KO mice (Fig. 4B), the expression of *UCP1*, *DIO2*, and *CPT1β* was significantly reduced in the IWAT and PRWAT of the cold-exposed FGF21-KO mice (Fig. 4C,D). Indeed, the induction of IWAT *UCP1* mRNA was reduced by nearly 50% in the FGF21-KO mice, compared with controls. In addition, FGF21 ablation resulted in reduced expression of genes that are indicative of browning (*Cox7a*, *Cox8b*, and *CIDEA*), suggesting that the adaptive browning of the perirenal and inguinal fat depot is impaired. This was also indicated by a large reduction in the amount of UCP1-positive multilocular adipocytes in the IWAT of the FGF21-KO mice (Fig. 4E). In EWAT, a fat depot that is not very responsive to cold stimulation and in which *FGF21* gene expression is not induced upon cold stimulation, the expression of thermogenic genes and tissue morphology was similar between control and knockout mice (Supplemental Fig. 2C). Taken together, these data show that FGF21 expression is required for normal adaptations to cold in thermogenically competent white fat pads.
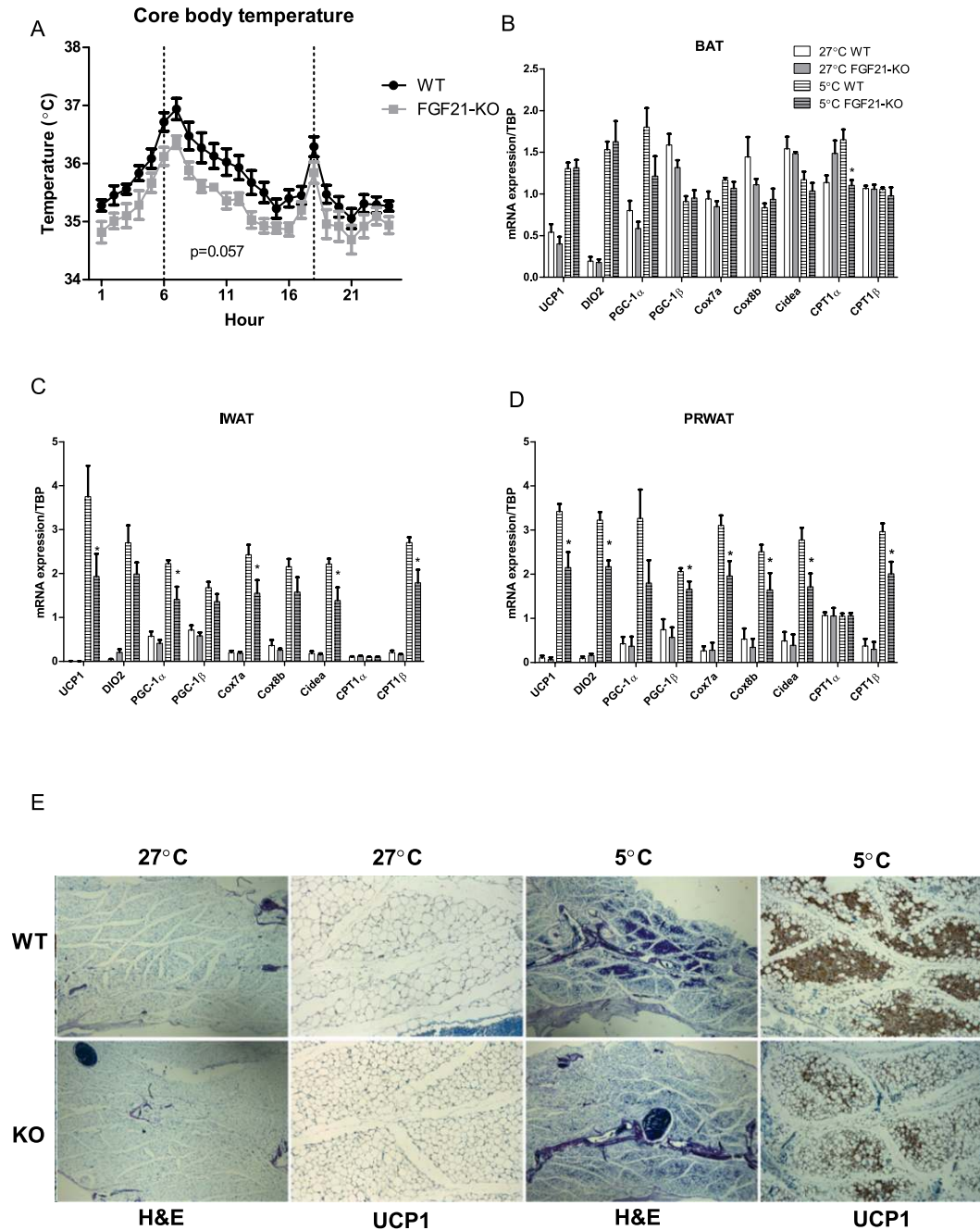
Figure 4. FGF21-KO display an impaired response to a cold challenge. Wild-type ($n = 5$) and FGF21-KO ($n = 5$) mice were implanted with activity- and temperature-measuring telemetry probes and were kept for a 72-h period at 5°C. (*A*) Diurnal core body temperature in wild-type and FGF21-KO mice. Real-time quantitative PCR analysis of thermogenic gene expression is shown from BAT (*B*), IWAT (*C*), and PRWAT (*D*). (*E*) H&E and UCP1 immunostaining in IWAT from wild-type and FGF21-KO mice. Data are shown ±SEM; 5°C wild type versus 5°C FGF21-KO, (*) $P < 0.05$.

PGC-1α is required for the thermogenic effect of FGF21 on adipose tissue

PGC-1α is a critical transcriptional regulator of oxidative metabolism and adaptive thermogenesis. PGC-1α itself is highly induced during cold exposure and has been found to coactivate many DNA-binding transcription factors required for thermogenesis, including PPARγ, PPARα, and ERRα. We therefore asked whether PGC-1α is required for the thermogenic effects of FGF21. Primary differentiated brown and inguinal adipocytes derived from fat-specific PGC-1α-KO (αFKO) and control PGC-1α Flox (αFlox) mice were treated with FGF21. As shown in Fig. 5, A and B, FGF21-induced expression of *UCP1*, *CIDEA*, and *CPT1β* was reduced in the absence of PGC-1α in both brown and inguinal white adipocytes. To investigate the
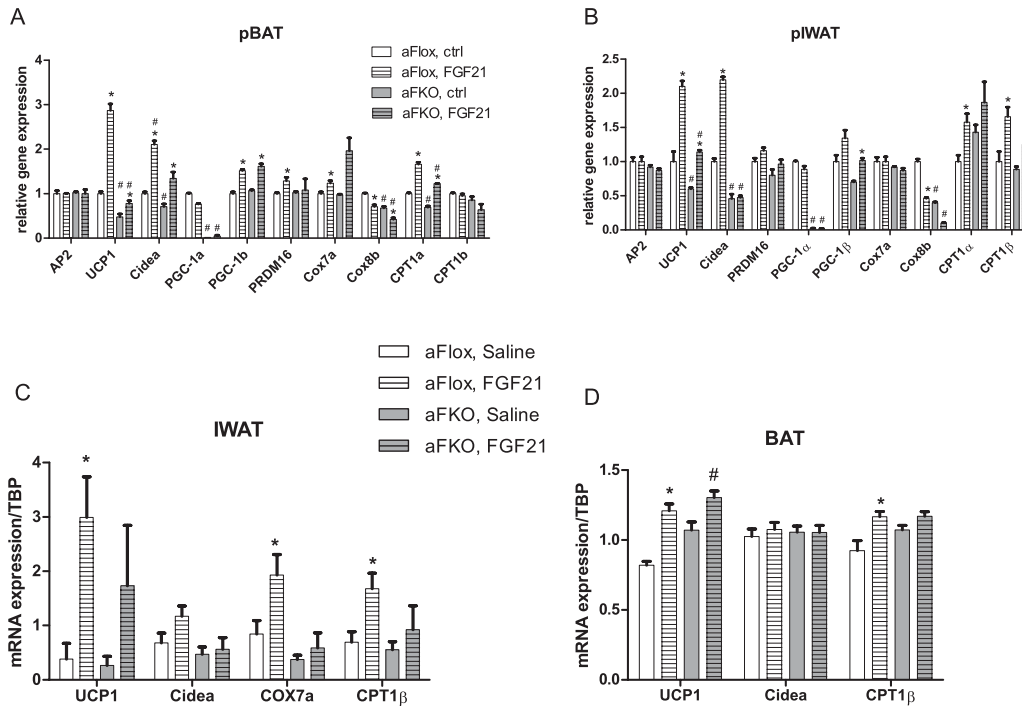
Fisher et al.

Figure 5. PGC-1α is required for the FGF21-mediated induction of thermogenic genes. To assess whether PGC-1α mediates the thermogenic effects of FGF21 in vitro, primary adipocytes sourced from αFKO mice were treated with FGF21 for 48 h. Real-time quantitative PCR analysis is shown from primary brown (*A*) and inguinal white (*B*) adipocytes. To test the effects in vivo, αFlox and αFKO mice were treated for 3 d with either saline or FGF21. mRNA expression of PGC-1α target genes is shown from IWAT (*C*) and BAT (*D*). Data are shown ±SEM. Saline (n = 8–9) versus FGF21 (n = 11–12), (*) $P < 0.05$; αFlox versus αFKO, (#) $P < 0.05$.

requirement of PGC-1α for this response in vivo, we treated αFKO mice with FGF21 for 3 d. Figure 5C illustrates that FGF21-mediated induction of thermogenic genes was attenuated in the IWAT of the αFKO mice. However, the response of BAT to FGF21 in the absence of PGC-1α was only marginally attenuated (Fig. 5D), although it should be noted that FGF21 induces *UCP1* expression to a far greater degree in IWAT. These data indicate that PGC-1α is required for the FGF21-induced thermogenic gene program in susceptible WATs.

FGF21 regulates PGC-1α at a post-transcriptional level in BAT and WAT

The regulation of PGC-1α during thermogenesis has mainly been studied and observed at the mRNA level. Although PGC-1α is clearly required for some FGF21-mediated effects on thermogenic gene expression, *PGC-1α* mRNA does not increase after 48 h of FGF21 treatment in culture (Fig. 2). In addition, we were not able to see any increase in *PGC-1α* mRNA level after 8 h and 24 h of FGF21 treatment (Supplemental Fig. 3A). The induction of *PGC-1α* mRNA by FGF21 in vivo is marginal, failing to reach significance in some of the depots. To investigate whether FGF21 preferentially alters the PGC-1α protein, we analyzed protein levels in cultured cells and in vivo. Indeed, in the primary BAT and IWAT adipocytes where no effect was observed on *PGC-1α* mRNA (Fig. 6A), a striking increase in PGC-1α protein was apparent with FGF21

treatment (Fig. 6B). In vivo, where FGF21 trended to increase *PGC-1α* mRNA in BAT and IWAT (Fig. 6C), PGC-1α protein levels were increased to a far greater extent (Fig. 6D). These data suggest that the role of FGF21 during cold exposure is to enhance PGC-1α protein levels within thermogenically active fat depots. This notion is further supported by the attenuated induction in PGC-1α protein content in the BAT and IWAT of FGF21-KO mice (Fig. 6F), despite little effect on mRNA expression (Fig. 6E).

To test the hypothesis that increased PGC-1α protein accumulation was due to enhanced protein stability, the turnover of PGC-1α protein was investigated with a cycloheximide chase experiment. Since PGC-1α protein levels are very low in brown and white differentiated adipocytes in culture, we used forced expression of adenoviral-driven *PGC-1α* in immortalized brown adipocytes (imBATs). As shown in Supplemental Figure 3B, FGF21 treatment enhanced thermogenic gene expression in these immortalized cells, similar to what we observed in primary adipocytes. In addition, despite similar levels of *PGC-1α* mRNA overexpression, higher amounts of PGC-1α protein were detected after FGF21 treatment (Supplemental Fig. 3C). However, the results show that PGC-1α protein stability was not increased in FGF21-treated adipocytes (Supplemental Fig. 3C,D). These data suggest that FGF21 regulates PGC-1α protein by post-translational mechanisms other than protein degradation.

Since FGF21 signaling results in Erk phosphorylation and activation (Fisher et al. 2011), we investigated whether
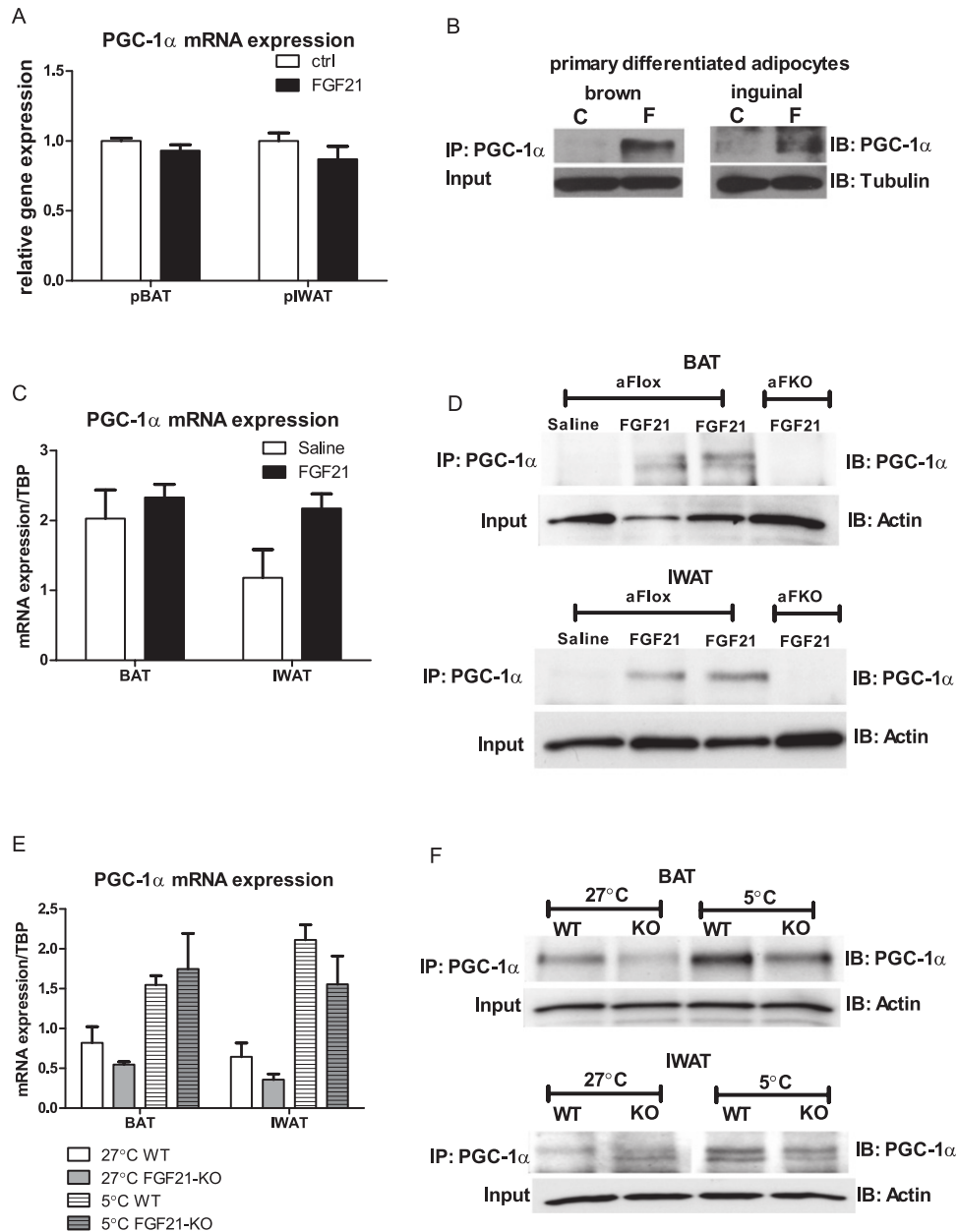
Figure 6. FGF21 regulates PGC-1α protein content of adipocytes in vitro and in vivo. In vitro PGC-1α mRNA (*A*) and protein (*B*) levels are shown from primary BAT and IWAT adipocytes treated with FGF21. In vivo PGC-1α mRNA (*C*) and protein (*D*) levels (*n* = 2 mice per lane) are shown from BAT and IWAT of FGF21-treated mice. In vivo PGC-1α mRNA (*E*) and protein (*F*) levels (*n* = 3 mice per lane) from BAT and IWAT of wild-type and FGF21-KO mice cold-exposed for 72 h. Data are shown ±SEM where applicable. (C) Control; (F) FGF21.

Erk activation is required for FGF21-mediated thermogenic gene expression and for the enhancement of PGC-1α protein levels. To this end, we treated imBATs with FGF21 in the absence and presence of the Erk inhibitor UO126. As the data in Supplemental Figure 3, E and F, show, neither FGF21-driven gene expression nor PGC-1α protein stabilization was suppressed by Erk inhibition.

Discussion

FGF21 has been described as an endocrine hormone with beneficial metabolic actions. We report here that adipose

FGF21 is a critical paracrine/autocrine-acting component of the endogenous cold response and is required for normal adaptations to cold exposure. *FGF21* expression is also necessary for the cold-induced recruitment of brown-like (beige) adipocytes in IWAT. In fact, pharmacologic doses of FGF21 are able to induce a thermogenic gene response in both BAT and thermogenically competent WAT depots. This process is associated with a large induction of PGC-1α protein with little effect on *PGC-1α* gene expression. FGF21 is the only known cold-induced secreted protein that functions to increase the appearance of brown-like/brite adipocytes in WAT depots. The lack of

alteration in circulating FGF21 upon cold exposure suggests that this factor acts on the adipose tissues via autocrine or paracrine signaling. Presumably, this evolved to expand the thermogenic machinery in vivo and provide a more robust defense against hypothermia than can be provided by the classically understood sympathetic nervous system–BAT pathway.

While the phenomenon of increased *FGF21* expression in BAT has been observed recently (Chartoumpekis et al. 2011; Hondares et al. 2011), little was known as to the function and importance of this process. In agreement with Hondares et al. (2010), we found that FGF21 can increase thermogenic gene expression, such as *UCP1* and *CIDEA*, in BAT and primary classical brown adipocytes. Interestingly, however, we found that FGF21 had far more profound effects on thermogenic gene expression in specific WAT depots (IWAT and PRWAT) that are thermogenically competent. Indeed, FGF21 appeared to induce the expression of many genes associated with the function of the brown/beige adipocytes. Furthermore, using immunostaining for UCP1, we found that this was due to a large increase in multilocular, brown-like adipocytes in the inguinal fat pads of the FGF21-treated mice.

FGF21 not only has the ability to induce a brown-like phenotype in WAT pharamologically, but is required for this physiological adaptation to occur during cold exposure. When cold-exposed, the FGF21-KO mice trended to be a little colder. Although pharmacologic doses of FGF21 enhance thermogenic gene expression in BAT, this process was not attenuated in the cold-exposed FGF21-KO mice, suggesting that compensation may be occurring in this tissue. Nevertheless, cold induction of thermogenic genes, including *UCP1* and other markers of brown-like adipocytes, was significantly attenuated in IWAT and PRWAT of FGF21-KO mice. When viewed in total, our data clearly show that FGF21 plays a far more important role in thermogenically competent WAT-containing tissue depots, such as inguinal subcutaneous and perirenal fat. In addition to adipose tissue thermogenesis, FGF21 may regulate lipolysis in vivo. However, the exact role of FGF21 in regulating lipolysis remains controversial, with reports of FGF21 both activating (Inagaki et al. 2007) and inhibiting (Arner et al. 2008; Li et al. 2009) this process in adipocytes. In the context of the time courses and treatment regimes that we used, we saw no evidence to suggest either scenario during FGF21-mediated thermogenesis (data not shown).

PGC-1α has been recognized as a critical regulator of thermogenesis and oxidative metabolism. It is therefore not completely surprising that this coactivator of transcription is important to the thermogenic effects of FGF21 both in culture and in vivo. This thermogenic response is not completely attenuated in the absence of PGC-1α and may be caused by redundancy to the second member of the PGC-1 family, PGC-1β. Most interesting, however, is the manner by which FGF21 regulates PGC-1α levels. Our data suggest that the role of FGF21 is mainly to increase PGC-1α protein rather than gene expression. Additionally, in cold-exposed knockout mice, the absence of FGF21

results in diminished PGC-1α protein levels, suggesting that this is an important function for FGF21 during a response to cold temperatures. How this occurs remains a subject of further investigation, but our experiments suggest that PGC-1α is not regulated on the level of protein stability. It is thus likely that other post-translational mechanisms, such as selective translation, may contribute.

The beneficial affects of FGF21 on glucose metabolism and body weight have evoked a substantial interest in FGF21 as a potential treatment for diseases such as obesity and diabetes (Coskun et al. 2008; Berglund et al. 2009; Xu et al. 2009). Our data support a clear function for FGF21 in regulating chronic adaptive thermogenesis by increasing the transcription of thermogenic genes and enhancing the thermogenic capacity of the organism by "browning" white fat. It is tempting to speculate that the thermogenic effects of FGF21 on adipose tissue may underlie many of its beneficial effects observed in vivo. Thermogenesis is intimately linked with energy expenditure and may explain the weight loss effects of FGF21 in mice. Further work will be required to delineate the role of adipose tissue thermogenesis in FGF21-mediated weight loss and glycemic control, and whether FGF21 could be used in the therapy of obesity.

Materials and methods

Animals

All studies were carried out using male C57Bl/6 mice obtained from The Jackson Laboratory and maintained on a 12:12-h light–dark cycle at 24°C. FGF21-KO mice were generated as previously described (Badman et al. 2009). Briefly, mice were generated by deletion of a 1200-base-pair (bp) region of FGF21, including the 3′ section of exon 1, all of exon 3, and the 5′ region of exon 3. Founders were then back-crossed 10 times onto a C57Bl6 background. αFKO mice were generated by crossing female mice homozygous for the floxed allele with heterozygous floxed male mice carrying a transgene expressing cre-recombinase under control of the adiponectin promoter. All animals were allowed ad libitum access to food unless otherwise stated. All studies were approved by the Beth Israel Deaconess Medical Center Institutional Animal Care and Use Committee.

Recombinant FGF21 protein

Recombinant FGF21 protein was generated by expression of human FGF21 in *Escherichia coli* and was subsequently refolded in vitro as previously described (Kharitonenkov et al. 2005).

Subcutaneous FGF21 infusion

FGF21 infusion for 3 d was delivered using Alzet miniosmotic pumps (Durect Corporation). Pumps were filled with either FGF21 (1 μg per hour; 24 μg per day) or vehicle (saline) and primed for 4–6 h at 37°C before implantation. The pump was inserted into the interscapular region under isoflurane anesthesia. Briefly, the surgical area was shaved and cleaned with povidone–iodine and an alcohol swab. A small lateral incision was made (10 mm) and the pump was carefully inserted. The incision was closed with silk sutures, and mice were allowed to recover from anesthesia in their home cages.

Cold exposure studies

Eleven-week-old wild-type and FGF21-KO mice were implanted with TA-F10 telemetry transmitters (Data Sciences International). Briefly, mice were anesthetized with isoflurane and their abdominal regions were shaved and prepped with betadine. A small vertical incision was then made in the center of the abdomen, and the peritoneal cavity was opened. A sterile telemetry probe was then carefully placed to one side of the peritoneum. The peritoneum was then closed with absorbable sutures before final closure of the abdomen with wound clips. Mice were allowed to recover from anesthesia in their home cages and were kept for a further 7 d at room temperature until recovery, and the wound clips were removed. Mice were then placed in an incubator for 6 d at 27°C before switching for a 72-h period to 5°C. Throughout this period, the telemetry probes were set to record the activity and core body temperature of the mice every minute. After 72 h of cold exposure, mice were euthanized and tissues were harvested. Temperature and activity data were analyzed by calculating the hourly average and binning each 24-h period. Statistics were analyzed via repeat measure ANOVA (GraphPad Software, Inc.).

Stromal–vascular (SV) culture and white adipocyte differentiation

Inguinal or epididymal SV fractions from 6- to 8-wk-old male mice were obtained by the following procedure. Dissected fat tissue from two or three mice (four to six fat pads total) was washed, minced, and then digested for 45 min at 37°C in PBS containing 10 mM CaCl, 2.4 U/mL dispase II (Roche), and 1.5 U/mL collagenase D (Roche). Digested tissue was then filtered through a 100-μm cell strainer to remove undigested tissues. The flow-through was then centrifuged at 600g for 5 min to pellet the SV cells. The SV cells, resuspended in complete SV culture medium (DMEM/F12 [1:1; Invitrogen] plus glutamax, pen/strep, and 10% FBS), were then filtered through a 40-μm cell strainer to remove clumps and large adipocytes. Following centrifugation as above, SV cells were then resuspended in SV culture medium and plated onto a 6-cm tissue culture dish.

For adipocyte differentiation assays, SV cells were plated and grown to confluence in SV culture medium. At confluence (day 0), cells were exposed to the adipogenic cocktail containing 1 μM dexamethasone, 5 μg/mL insulin, 0.5 mM isobutylmethylxanthine (DMI), and 1 μM rosiglitazone in SV culture medium. Forty-eight hours after induction, cells were maintained in SV culture medium containing 5 μg/mL insulin. At day 6 of differentiation, cells were treated for two consecutive days with 50 nM FGF21 and harvested at day 8. For isoproteranol treatments, cells were treated with 1–5 μM isoprperanol for 6–8 h.

SV culture and brown adipocyte differentiation

The interscapular brown fat pad (total of six to eight fat pads) was dissected from newborn mice (postnatal days 2–4), minced, and then digested for 45 min at 37°C in isolation buffer (123 mM NaCl, 5 mM KCl, 1.3 mM CaCl$_2$, 5.0 mM glucose, 100 mM HEPES, 4% BSA, 1.5 mg/mL collagenase B [Roche]). Digested tissue was then filtered through a 100-μm cell strainer to remove undigested tissues. The flow-through was then centrifuged at 600g for 10 min to pellet the SV cells. The SV cells were then resuspended in complete SV culture medium (DMEM/F12 [1:1; Invitrogen] plus glutamax, pen/strep, and 10% FBS) and plated onto a 10-cm tissue culture dish.

For brown adipocyte differentiation assays, SV cells were plated and grown to confluence in SV culture medium. At confluence (day 0), cells were exposed to the adipogenic cocktail containing 5 μM dexamethasone, 0.02 μM insulin, 0.5 mM isobutylmethyl-

xanthine, 1 nM T3, 125 μM indomethacin, and 1 μM rosiglitazone in SV culture medium. Forty-eight hours after induction, cells were maintained in SV culture medium containing 0.02 μM insulin and 1 nM T3. At day 6 of differentiation, cells were treated for two consecutive days with 50 nM FGF21 and harvested at day 8. For isoproteranol treatments, cells were treated with 1–5 μM isoprperanol for 6–8 h.

For differentiation of imBATs, preadipocytes were plated at a density that allowed them to grow to confluence within 24–48 h. At confluence, cells were differentiated using the above-described brown fat differentiation cocktail. At day 6 of differentiation, cells were treated for two consecutive days with 50 nM FGF21 and harvested at day 8. For adenoviral infections, adipocytes were transduced overnight at day 5 of differentiation with 1×10^6 plaque-forming units (pfu) per 10-cm dish of PGC-1α-expressing virus. For the cyclohexamide chase, adipocytes were infected with PGC-1α adenovirus, treated for 2 d with FGF21, and subsequently incubated in medium containing 20 μg/mL cycloheximide. Cells were harvested at the indicated time points, and cell lysates were applied for Western blotting. β-Tubulin was used for loading control. The quantification of the signal intensity was done using ImageJ software. To block Erk activation, differentiated adipocytes (day 6) were simultaneously incubated with 50 nM FGF21 and 10 μM UO126 until harvesting.

RNA isolation and real-time PCR analysis

Total RNA from cultured cells or mouse tissues was isolated by Qiazol extraction and purification using Qiagen RNeasy minicolumns according to the manufacturer's instructions (Qiagen). For quantitative real-time PCR analysis, 1–1.5 μg of total RNA was reverse-transcribed using the High Capacity cDNA Reverse Transcription kit (Applied Biosystems). SYBR Green reactions using the SYBR Green PCR Master mix (Applied Biosystems) were assembled along with 250 nM primers according to the manufacturer's instructions and were performed using an ABI 7900 HT machine. Relative expression of mRNAs was determined after normalization to Rps18 or TBP. Student's t-test was used to evaluate statistical significance. All primer sequences are available on request.

Immunoprecipitation and Western blot analysis

Whole-cell extracts were prepared from cells by homogenization in lysis buffer containing 50 mM Tris (pH 7.4), 500 mM NaCl, 1% NP40, 20% glycerol, and 1 mM DTT, supplemented with protease inhibitor cocktail (Roche Diagnostics Corporation). For immunoprecipitation, the lysate was diluted 1:5 with an immunoprecipitation buffer containing 50 mM Tris, 150 mM KCL, 20% glycerol, and 2 mM EDTA. Two milligrams of diluted total protein lysate was incubated overnight at 4°C with 2 μg of anti-PGC-1α antibody (Santa Cruz Biotechnology). The next morning, 20 μL of equilibrated Sepharose beads were added, followed by an additional 4 h of incubation at 4°C. The beads were then washed five times with 1 mL of immunoprecipitation buffer, resuspended in Laemmli buffer, separated by SDS-PAGE, and transferred to an immobilon P membrane (Millipore). For PGC-1α immunoblots, membranes were blocked in 5% milk/0.1% Tween in PBS for >1 h and then incubated for 2 h at room temperature with anti-PGC-1α monoclonal antibody (EMD) diluted 2 μg/mL in 3% BSA/0.1% Tween in PBS. Proteins were visualized using the Supersignal West Dura HRP Detection kit (Pierce).

Immunohistochemistry

For histological analysis, adipose tissue was fixed in 4% formaldehyde, embedded in paraffin, and cut to 6-μm sections on slides.

Immunohistochemistry was performed using the Vectastain Elite ABC kit according to the manufacturer's instructions using rabbit UCP1 antibodies (1:1000).

Acknowledgments

References

Arner P, Pettersson A, Mitchell PJ, Dunbar JD, Kharitonenkov A, Ryden M. 2008. FGF21 attenuates lipolysis in human adipocytes—a possible link to improved insulin sensitivity. *FEBS Lett* **582:** 1725–1730.

Badman MK, Pissios P, Kennedy AR, Koukos G, Flier JS, Maratos-Flier E. 2007. Hepatic fibroblast growth factor 21 is regulated by PPARα and is a key mediator of hepatic lipid metabolism in ketotic states. *Cell Metab* **5:** 426–437.

Badman MK, Koester A, Flier JS, Kharitonenkov A, Maratos-Flier E. 2009. Fibroblast growth factor 21-deficient mice demonstrate impaired adaptation to ketosis. *Endocrinology* **150:** 4931–4940.

Barbatelli G, Murano I, Madsen L, Hao Q, Jimenez M, Kristiansen K, Giacobino JP, De Matteis R, Cinti S. 2010. The emergence of cold-induced brown adipocytes in mouse white fat depots is determined predominantly by white to brown adipocyte transdifferentiation. *Am J Physiol Endocrinol Metab* **298:** E1244–E1253. doi: 10.1152/ajpendo.00600.2009.

Barbera MJ, Schluter A, Pedraza N, Iglesias R, Villarroya F, Giralt M. 2001. Peroxisome proliferator-activated receptor α activates transcription of the brown fat uncoupling protein-1 gene. A link between regulation of the thermogenic and lipid oxidation pathways in the brown fat cell. *J Biol Chem* **276:** 1486–1493.

Berglund ED, Li CY, Bina HA, Lynes SE, Michael MD, Shanafelt AB, Kharitonenkov A, Wasserman DH. 2009. Fibroblast growth factor 21 controls glycemia via regulation of hepatic glucose flux and insulin sensitivity. *Endocrinology* **150:** 4084–4093.

Cannon B, Nedergaard J. 2011. Nonshivering thermogenesis and its adequate measurement in metabolic studies. *J Exp Biol* **214:** 242–253.

Cederberg A, Gronning LM, Ahren B, Tasken K, Carlsson P, Enerback S. 2001. FOXC2 is a winged helix gene that counteracts obesity, hypertriglyceridemia, and diet-induced insulin resistance. *Cell* **106:** 563–573.

Chartoumpekis DV, Habeos IG, Ziros PG, Psyrogiannis AI, Kyriazopoulou VE, Papavassiliou AG. 2011. Brown adipose tissue responds to cold and adrenergic stimulation by induction of FGF21. *Mol Med* **17:** 736–740.

Christian M, Kiskinis E, Debevec D, Leonardsson G, White R, Parker MG. 2005. RIP140-targeted repression of gene expression in adipocytes. *Mol Cell Biol* **25:** 9383–9391.

Cinti S. 2009. Reversible physiological transdifferentiation in the adipose organ. *Proc Nutr Soc* **68:** 340–349.

Coskun T, Bina HA, Schneider MA, Dunbar JD, Hu CC, Chen Y, Moller DE, Kharitonenkov A. 2008. FGF21 corrects obesity in mice. *Endocrinology* **149:** 6018–6027.

Cousin B, Cinti S, Morroni M, Raimbault S, Ricquier D, Penicaud L, Casteilla L. 1992. Occurrence of brown adipocytes in rat white adipose tissue: Molecular and morphological characterization. *J Cell Sci* **103:** 931–942.

Feldmann HM, Golozoubova V, Cannon B, Nedergaard J. 2009. UCP1 ablation induces obesity and abolishes diet-induced thermogenesis in mice exempt from thermal stress by living at thermoneutrality. *Cell Metab* **9:** 203–209.

Fisher FM, Chui PC, Antonellis PJ, Bina HA, Kharitonenkov A, Flier JS, Maratos-Flier E. 2010. Obesity is an FGF21 resistant state. *Diabetes* **59:** 2781–2789.

Fisher FM, Estall JL, Adams AC, Antonellis PJ, Bina HA, Flier JS, Kharitonenkov A, Spiegelman BM, Maratos-Flier E. 2011. Integrated regulation of hepatic metabolism by fibroblast growth factor 21 (FGF21) in vivo. *Endocrinology* **152:** 2996–3004.

Ghorbani M, Himms-Hagen J. 1997. Appearance of brown adipocytes in white adipose tissue during CL 316,243-induced reversal of obesity and diabetes in Zucker fa/fa rats. *Int J Obes Relat Metab Disord* **21:** 465–475.

Hansen JB, Jorgensen C, Petersen RK, Hallenborg P, De Matteis R, Boye HA, Petrovic N, Enerback S, Nedergaard J, Cinti S, et al. 2004. Retinoblastoma protein functions as a molecular switch determining white versus brown adipocyte differentiation. *Proc Natl Acad Sci* **101:** 4112–4117.

Hondares E, Rosell M, Gonzalez FJ, Giralt M, Iglesias R, Villarroya F. 2010. Hepatic FGF21 expression is induced at birth via PPARα in response to milk intake and contributes to thermogenic activation of neonatal brown fat. *Cell Metab* **11:** 206–212.

Hondares E, Iglesias R, Giralt A, Gonzalez FJ, Giralt M, Mampel T, Villarroya F. 2011. Thermogenic activation induces FGF21 expression and release in brown adipose tissue. *J Biol Chem* **286:** 12983–12990.

Inagaki T, Dutchak P, Zhao G, Ding X, Gautron L, Parameswara V, Li Y, Goetz R, Mohammadi M, Esser V, et al. 2007. Endocrine regulation of the fasting response by PPARα-mediated induction of fibroblast growth factor 21. *Cell Metab* **5:** 415–425.

Johnson CL, Weston JY, Chadi SA, Fazio EN, Huff MW, Kharitonenkov A, Koester A, Pin CL. 2009. Fibroblast growth factor 21 reduces the severity of cerulein-induced pancreatitis in mice. *Gastroenterology* **137:** 1795–1804.

Kharitonenkov A, Shiyanova TL, Koester A, Ford AM, Micanovic R, Galbreath EJ, Sandusky GE, Hammond LJ, Moyers JS, Owens RA, et al. 2005. FGF-21 as a novel metabolic regulator. *J Clin Invest* **115:** 1627–1635.

Kopecky J, Clarke G, Enerback S, Spiegelman B, Kozak LP. 1995. Expression of the mitochondrial uncoupling protein gene from the aP2 gene promoter prevents genetic obesity. *J Clin Invest* **96:** 2914–2923.

Lepper C, Fan CM. 2010. Inducible lineage tracing of Pax7-descendant cells reveals embryonic origin of adult satellite cells. *Genesis* **48:** 424–436.

Li X, Ge H, Weiszmann J, Hecht R, Li YS, Veniant MM, Xu J, Wu X, Lindberg R, Li Y. 2009. Inhibition of lipolysis may contribute to the acute regulation of plasma FFA and glucose by FGF21 in ob/ob mice. *FEBS Lett* **583:** 3230–3234.

Lowell BB, S-Susulic V, Hamann A, Lawitts JA, Himms-Hagen J, Boyer BB, Kozak LP, Flier JS. 1993. Development of obesity in transgenic mice after genetic ablation of brown adipose tissue. *Nature* **366:** 740–742.

Moyers JS, Shiyanova TL, Mehrbod F, Dunbar JD, Noblitt TW, Otto KA, Reifel-Miller A, Kharitonenkov A. 2007. Molecular determinants of FGF-21 activity-synergy and cross-talk with PPARγ signaling. *J Cell Physiol* **210:** 1–6.

Petrovic N, Walden TB, Shabalina IG, Timmons JA, Cannon B, Nedergaard J. 2010. Chronic peroxisome proliferator-activated receptor γ (PPARγ) activation of epididymally derived white adipocyte cultures reveals a population of thermogenically competent, UCP1-containing adipocytes molecularly distinct from classic brown adipocytes. *J Biol Chem* **285:** 7153–7164.

Potthoff MJ, Inagaki T, Satapati S, Ding X, He T, Goetz R, Mohammadi M, Finck BN, Mangelsdorf DJ, Kliewer SA, et al. 2009. FGF21 induces PGC-1α and regulates carbohydrate and fatty acid metabolism during the adaptive starvation response. *Proc Natl Acad Sci* **106:** 10853–10858.

Romanatto T, Roman EA, Arruda AP, Denis RG, Solon C, Milanski M, Moraes JC, Bonfleur ML, Degasperi GR, Picardi PK, et al. 2009. Deletion of tumor necrosis factor-α receptor 1 (TNFR1) protects against diet-induced obesity by means of increased thermogenesis. *J Biol Chem* **284:** 36213–36222.

Seale P, Bjork B, Yang W, Kajimura S, Chin S, Kuang S, Scime A, Devarakonda S, Conroe HM, Erdjument-Bromage H, et al. 2008. PRDM16 controls a brown fat/skeletal muscle switch. *Nature* **454:** 961–967.

Seale P, Conroe HM, Estall J, Kajimura S, Frontini A, Ishibashi J, Cohen P, Cinti S, Spiegelman BM. 2011. Prdm16 determines the thermogenic program of subcutaneous white adipose tissue in mice. *J Clin Invest* **121:** 96–105.

Tsukiyama-Kohara K, Poulin F, Kohara M, DeMaria CT, Cheng A, Wu Z, Gingras AC, Katsume A, Elchebly M, Spiegelman BM, et al. 2001. Adipose tissue reduction in mice lacking the translational inhibitor 4E-BP1. *Nat Med* **7:** 1128–1132.

Wang H, Zhang Y, Yehuda-Shnaidman E, Medvedev AV, Kumar N, Daniel KW, Robidoux J, Czech MP, Mangelsdorf DJ, Collins S. 2008. Liver X receptor α is a transcriptional repressor of the uncoupling protein 1 gene and the brown fat phenotype. *Mol Cell Biol* **28:** 2187–2200.

Wente W, Efanov AM, Brenner M, Kharitonenkov A, Koster A, Sandusky GE, Sewing S, Treinies I, Zitzer H, Gromada J. 2006. Fibroblast growth factor-21 improves pancreatic β-cell function and survival by activation of extracellular signal-regulated kinase 1/2 and Akt signaling pathways. *Diabetes* **55:** 2470–2478.

Wu Z, Puigserver P, Andersson U, Zhang C, Adelmant G, Mootha V, Troy A, Cinti S, Lowell B, Scarpulla RC, et al. 1999. Mechanisms controlling mitochondrial biogenesis and respiration through the thermogenic coactivator PGC-1. *Cell* **98:** 115–124.

Xu J, Lloyd DJ, Hale C, Stanislaus S, Chen M, Sivits G, Vonderfecht S, Hecht R, Li YS, Lindberg RA, et al. 2009. Fibroblast growth factor 21 reverses hepatic steatosis, increases energy expenditure, and improves insulin sensitivity in diet-induced obese mice. *Diabetes* **58:** 250–259.

FGF21 regulates PGC-1α and browning of white adipose tissues in adaptive thermogenesis

ffolliott M. Fisher, Sandra Kleiner, Nicholas Douris, et al.

Supplemental Material	http://genesdev.cshlp.org/content/suppl/2012/02/01/26.3.271.DC1
References	This article cites 38 articles, 12 of which can be accessed free at: http://genesdev.cshlp.org/content/26/3/271.full.html#ref-list-1
License	
Email Alerting Service	Receive free email alerts when new articles cite this article - sign up in the box at the top right corner of the article or **click here.**